Helium Ash Exhaust Studies with Core Fueling by a Helium Beam: *L*-Mode Divertor Discharges with Neutral-Beam Heating in the JT-60 Tokamak

H. Nakamura, T. Hirayama, Y. Koide, K. Tobita, K. Tani, T. Fukuda, H. Kubo, M. Kuriyama, Y. Kusama, A. Sakasai, T. Sugie, and H. Yoshida

Japan Atomic Energy Research Institute, Naka Fusion Research Establishment, Naka-machi, Naka-gun, Ibaraki-ken 311-01, Japan

(Received 8 October 1990)

The first experiment simulating helium ash exhaust in a DT fusion reactor has been performed in the JT-60 tokamak with *L*-mode divertor discharges. He was injected with a 30-keV neutral beam to realize core fueling. Divertor neutral pressures of hydrogen and He increased in proportion to the cube of the electron density of the main plasma. The He enrichment factor was 0.5 at $\bar{n}_e = 6\times10^{19}$ m^{-3} and increased in proportion to n_e. In an *L*-mode plasma of a fusion reactor, thermalized α particles (He ash) generated in the core plasma can be easily exhausted with a pumping speed of several tens m^3/s.

PACS numbers: 52.50.Gj, 52.55.Fa, 52.70.Nc

In a burning fusion plasma with deuterium (D) and tritium (T) fuels, 3.5-MeV α particles are generated in the D-T reaction. After thermalization, the α particles become helium ash. The concentration of the He ash must be controlled within a permissible level to prevent fuel dilution and quenching of the burning plasma. For example, this level is about 10% in ITER (International Thermonuclear Experimental Reactor) [1]. Therefore, control of the He ash is one of the critical issues in tokamak experiments. In previous experiments, He ash exhaust was studied in the Ohmically heated D-III tokamak [2,3], and He transport in the PDX tokamak [4]. Recently, more precise studies have been reported from the TFTR [5] and TEXTOR [6] tokamaks. However, in the above experiments, He gas was introduced from the plasma edge by gas puffing. In the case of a fusion reactor, the birth profile of the He ash has a centrally peaked shape [7]. The effect of location of the He source on the He ash behavior is not yet understood. Therefore, for reliable design of a fusion reactor, an experiment simulating the birth profile is necessary. This paper presents the first experiment of He ash exhaust with core fueling by a He beam in neutral-beam- (NB-) heated *L*-mode discharges of the JT-60 tokamak. Also, an experiment with edge fueling by He gas puffing has been done.

The JT-60 device is a large tokamak with a single-null poloidal divertor at the bottom of the torus. Typical parameters are a major radius of 2.9 m, a minor radius of 0.7 m, a plasma current of 1 MA, a toroidal field of 4.5 T, and a discharge duration of 10 s. Hydrogen plasmas are heated for 4 s by a hydrogen NB with heating powers of 10 to 18 MW and with a beam energy of 70 keV. A He NB with a fueling rate of 0.27 Pa m^3/s is injected for 2 s with a beam energy of 30 keV. In a He beam-line chamber, a cryopump cooled by liquid He is specially condensed by SF_6 gas to pump He gas. In the case of He gas fueling, He is puffed with a fueling rate of 0.5 Pa m^3/s for 3 s. In the divertor region, the neutral-particle pressures of hydrogen and He are measured during a discharge by a magnetically shielded residual-gas mass analyzer (RGA) with a scanning time of 0.1 s. The intensities of H_β and He II (4686 Å) emissions are measured by a spectrometer with a viewing angle around the *X* point and the divertor plate. In the main plasma, spatial profiles of electron density and electron temperature are measured with a multichannel Thomson scattering system. A far-infrared interferometer viewing along an off-axis vertical chord ($r = 0.4a$) is used for measurement of the line-integral electron density of the main plasma, where a is the minor plasma radius. Charge-exchange recombination spectroscopy (CXRS) is used to measure the He^{2+}-ion density profile in the main plasma by observing the transition at 4686 Å ($n = 4 \rightarrow 3$) of He^+. In addition to the He transport analysis, these CXRS data are used to calibrate the He particle density evaluated by $\Delta\bar{n}_e/2$ in the He exhaust study, where $\Delta\bar{n}_e$ is the increment of the line-averaged electron density after the He fueling. In the case of He gas fueling, the He particle density of the central region is also measured using a double CX reaction by injecting a He probe beam with a beam energy of 160 keV [8].

Typical wave forms in the He beam fueling experiments are shown in Fig. 1. During the He beam injection, the increase of the line-averaged electron density (n_e) is observed in Fig. 1(a). Solid and dashed lines depict n_e with and without the He beam fueling, respectively. The increment of the electron density is caused by the He beam fueling. In the soft-x-ray signal, the sawtooth period was around 180 ms both with and without He beam fueling. A clear difference of MHD behavior was not observed. Figure 1(b) shows the H_β and He II (4686 Å) emissions in the divertor region. Since significant change of the H_β emission is not observed after the He beam injection, an enhancement of hydrogen recycling by the He beam can be neglected. Figures 1(c) and 1(d) show the spatial profiles of the electron density and the electron temperature measured by Thomson scattering, and the He^{2+} ion density by CXRS. In Fig. 1(d), the

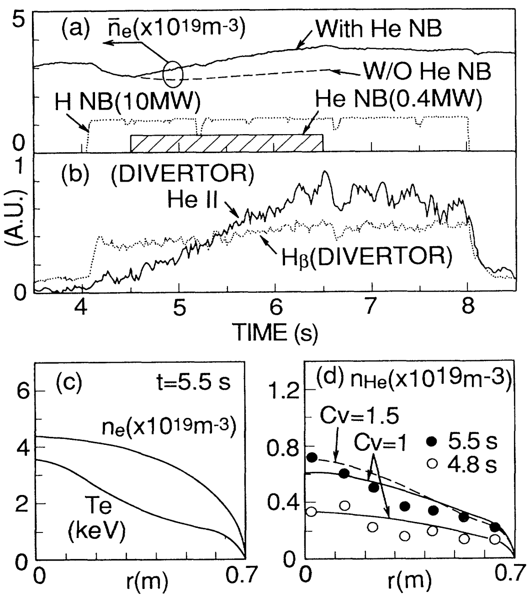

FIG. 1. Time histories from a typical He beam fueling discharge for a 1-MA plasma current. (a) Line-averaged electron densities $\bar{n}_e$ with and without the He beam fueling. (b) H_β and He II intensities in the divertor. (c) Electron temperature and electron density profiles. (d) He particle density profiles. Open and solid circles are measured values with CXRS. Solid lines are calculated by transport code.

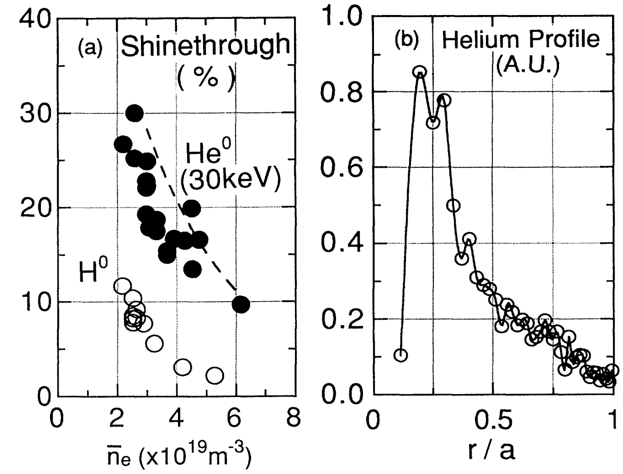

FIG. 2. (a) Shinethrough of the He and hydrogen beams as a function of line-averaged electron density n_e. Dashed line is calculated shinethrough of the He beam by the Monte Carlo code. (b) Calculated deposition profile of helium neutral beam. He beam energy = 30 keV, $\bar{n}_e = 4.5\times10^{19}$ m^{-3}, $T_e(0) = 3$ keV, $Z_{\rm eff} = 2$. Solid line is shown by spline interpolation.

solid lines are spatial profiles of the He particle densities calculated by a one-dimensional time-dependent transport code [9]. The peaking factor C_v is defined by the inward flow velocity $v_{\rm in} = -C_v D_a 2r/a^2$. D_a is a spatially uniform anomalous diffusion coefficient of 0.4 m^2/s, determined by comparing the computed central He^{2+} density with the measured one [10]. C_v of the He^{2+} is in the range of 1 to 1.5. On the other hand, C_v of the bulk plasma is in the range of 0 to 1. These results show that the He has a slightly more peaked density profile than the bulk plasma. So, in the estimation of the line-averaged particle densities of He and electrons, these spatial profiles are used. In Fig. 1(b), prior to the He beam injection, a small amount of He II emission is observed. This implies that the He implanted into the graphite tiles in previous shots is desorbed by hydrogen NB injection. The He particle density ($\bar{n}_{\rm He}$) in the main plasma consists of an incremental particle density after the He fueling ($\Delta\bar{n}_{\rm He}$) and a background particle density without the He fueling ($\bar{n}_{\rm He}^{\rm BG}$). In the range $\bar{n}_e = 3\times10^{19}$ m^{-3} to 4×10^{19} m^{-3}, $\bar{n}_{\rm He}^{\rm BG}/\Delta\bar{n}_{\rm He}$ is estimated to be about 20%. According to the He II emission ($I_{\rm He\,II}$), there is no clear density dependence of $I_{\rm He\,II}^{\rm BG}/\Delta I_{\rm He\,II}$. Therefore, $1.2\times\Delta\bar{n}_{\rm He}$ is used as $\bar{n}_{\rm He}$ assuming 20% of background He. For analysis, the data after 2 s from the start of the He fueling are used.

Core fueling by the He beam is confirmed by measurement of shinethrough (ST) of the NB and by calculation of the deposition profile. Figure 2(a) shows ST measured by a thermocouple array attached to inner graphite tiles. Open circles show ST of a 40-keV hydrogen NB in a different experiment. ST of the He beam is larger by a factor of 3 than that of the hydrogen beam. These results indicate that the He beam can be deposited into the core plasma. The dashed line is the calculated ST by an orbit-following Monte Carlo (OFMC) code [7]. There is good agreement between the measured ST and the calculated one. The calculated deposition profile of the He beam is shown in Fig. 2(b). The plasma parameters were $\bar{n}_e = 4.5\times10^{19}$ m^{-3}, $T_e(0) = 3$ keV, and $Z_{\rm eff} = 2$. The off-axis peak position of the deposition profile arises from off-axis injection. In this case, the predicted ST is 17.5%. Good agreement between the calculation and the measurement implies that core fueling of the He beam is reliable. Although ST of the He beam becomes thermal He neutrals, these are negligible as compared with recycling flux from the divertor region. Gilbody *et al.* [11] show that the fraction of metastables in the He NB is less than 1% for a He neutralizer at equilibrium conditions. Since a He neutralizer was used in our experiment, metastable He can be considered negligible.

For efficient He ash exhaust, high neutral-particle pressure of He in the divertor is necessary. Figure 3(a) shows the neutral pressures of hydrogen (P_{H_2}) and He ($P_{\rm He}$) in the divertor as the function of n_e in the hydrogen NB-heated discharges with the He beam fueling. In Fig. 3(b), above $\bar{n}_e = 4\times10^{19}$ m^{-3}, the ratio of the He particle density to the electron density in the main plasma is in the permissible range of concentration of the He ash. In a fusion reactor, the permissible concentration can be achieved by an appropriate pumping system depending on

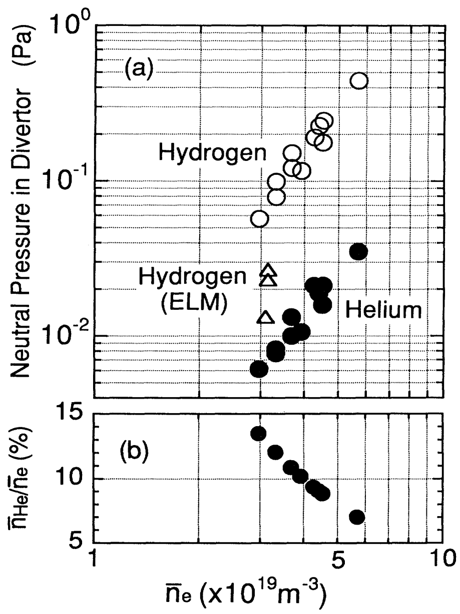

FIG. 3. (a) Neutral pressures of helium and hydrogen as a function of the line-averaged electron density of the main plasma. $P_{NB}=10$ to 17 MW, $I_p=1$ MA. Open and solid circles are neutral pressures in the *L*-mode discharges. Open triangles are hydrogen neutral pressure in *H* mode. (b) Ratio of helium density to electron density in the main plasma.

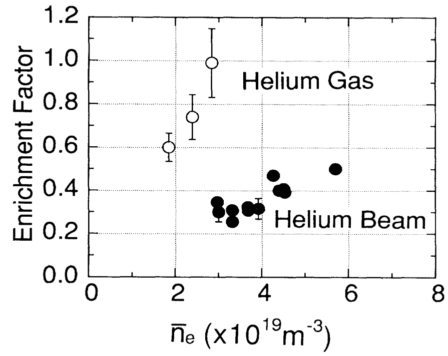

FIG. 4. He enrichment factor η as a function of the line-averaged electron density in the NB-heated divertor discharges of $P_{NB}=10$ to 17 MW and $I_p=1$ MA. Open and solid circles are η in He gas fueling and He beam fueling.

the transport behavior of He. The maximum neutral-particle pressures attained in this experiment are $P_{H_2}=0.43$ Pa and $P_{He}=0.036$ Pa at $\bar{n}_e=5.8\times10^{19}$ m^{-3}, respectively. Both pressures increase approximately in proportion to n_e^3. A similar dependence was also observed in the intensities of H_β and He II (4686 Å) emissions in the divertor. In the case of Ohmically heated discharges with He gas fueling [12], a clear dependence of P_{He} on n_e was not observed, whereas P_{H_2} increased in proportion to n_e^3. These results suggest that high heating power is necessary to localize He in the divertor. Using a two-point divertor model [13], the localization of He in the NB-heated discharges is explained. The particle confinement time of $\tau_P=20$ ms is used from the previous experiment of JT-60 [14]. At $\bar{n}_e=3\times10^{19}$ m^{-3}, the particle flux is calculated to be 3×10^{22} s^{-1}. Also, a particle multiplication factor of 20 is used because the ratio of P_{H_2} in the divertor to that in the main plasma is about 20. As a result, the divertor plasma parameters are estimated to be an electron temperature of 10 eV and an electron density of 3×10^{20} m^{-3} at $\bar{n}_e=3\times10^{19}$ m^{-3}. Using these values, the mean free path of He, defined as $\lambda=v/\bar{n}_e\langle\sigma v\rangle$, is calculated to be about 0.004 to 0.04 m in the divertor plasma, where the particle velocity of detrapped He is $v=(0.1-1)\times10^4$ m/s for 0.02 to 2 eV and the electron impact ionization reaction rate [15] is $\langle\sigma v\rangle=8\times10^{-16}$ m^3/s for 10 eV. Considering the half-width of the divertor heat flux profile measured by an infrared camera (4 cm), the characteristic divertor dimension is around 10 cm. Therefore, He particles can be trapped in the divertor plasma and localization of the He particles is expected. These results demonstrate that thermalized α particles (He ash) generated in the core plasma can be easily exhausted to the divertor region in an *L*-mode plasma. On the other hand, in an *H*-mode discharge, He ash exhaust is a crucial item because the neutral-particle pressure in the divertor decreases due to good particle confinement. For example, P_{H_2} in *H*-mode discharges with ELMs (edge localized modes) is $\frac{1}{3}$ to $\frac{1}{2}$ of that in the *L* mode as shown in Fig. 3(a). Therefore, it is expected that P_{He} in the *H* mode is also lower than in the *L* mode.

Another key issue in the He ash exhaust is the ratio of the He particle density to the hydrogen one in the divertor. A high concentration of He is desirable. To evaluate this characteristic, the enrichment factor η was defined as $(P_{He}/2P_{H_2})^{div}/(\bar{n}_{He}/\bar{n}_e)^{main}$ in the previous studies [2,3]. Figure 4 shows η as a function of n_e of the main plasma in the NB-heated discharges with $P_{NB}=10$ to 17 MW. In the case of core fueling, η is 0.25 to 0.5 for $\bar{n}_e=(2.9-5.8)\times10^{19}$ m^{-3}. For data points with error bars, n_{He} was measured with CXRS. The uncertainty in η is mainly caused by the CXRS measurement. Although He enrichment in the divertor is not observed, η increases in proportion to n_e. This dependence can be explained quantitatively by the n_e dependence of each parameter in the equation for η, where $P_{H_2}\propto n_e^3$, $P_{He}\propto n_e^3$, and n_{He} is nearly constant. This characteristic of η is promising for efficient He ash exhaust in high-density operation. On the other hand, in the case of edge fueling by He gas puffing, η is higher than with He beam fueling, being 0.6 to 0.98 for $\bar{n}_e=(1.9-2.8)\times10^{19}$ m^{-3}. In this case, the uncertainty in η is caused by the estimation of $\Delta\bar{n}_e$. This high η can be explained by the difference in fueling efficiency defined by $[(dN_{He}/dt)_{-0}-(dN_{He}/dt)_{+0}]/Q_{He}$, where Q_{He} is the He fueling rate, and $(dN_{He}/dt)_{-0}$ and

$(dN_{He}/dt)_{+0}$ are time derivatives of the number of He atoms before and after the He fueling termination, respectively. The fueling efficiency in the He beam is about 100%. On the other hand, in the case of He gas, it is 40% to 50%. In this case, the ratio of the He neutral pressure to the hydrogen one is 1.7 times higher than that in the He beam. A possible reason for this high concentration of He is that He gas injected into a vacuum chamber is easily shielded by a boundary plasma and retained in the divertor region. These results show that core fueling by a He beam is essential for simulating He ash behavior in plasma with high NB heating power.

Based on these results, the required pumping speed of the He ash exhaust (S_p) in L-mode discharges can be estimated. For example, in the case of a fusion reactor like ITER, the He ash generation rate (Q_{He}) is 1.4 Pa m^3/s. Using the definition of η, P_{He}^{div} is calculated by $2\eta(n_{He}/n_e)^{main}P_{H_2}^{div}$. Extrapolating the JT-60 result, $P_{H_2}^{div}$ is assumed to be around 1 Pa at $\bar{n}_e = 1\times10^{20}$ m^{-3}. Using an η of 0.5 and the permissible He ash concentration of 10%, P_{He}^{div} is estimated to be 0.1 Pa. So, S_p ($=Q_{He}/P_{He}^{div}$) is calculated to be 14 m^3/s. Considering experimental ambiguities, S_p should be around several tens of m^3/s in the L-mode discharges.

In summary, He ash exhaust with core fueling by a He beam was demonstrated in the NB-heated divertor discharges of the JT-60 tokamak. P_{H_2} and P_{He} increase with n_e^3. The He enrichment factor η is 0.25 to 0.5 and increases with $\bar{n}_e$. Core fueling by the He beam is essential for simulating He ash behavior in a fusion reactor. These results show that in the case of L-mode discharges, thermalized α particles (He ash) generated in the core plasma can be easily exhausted in a fusion reactor.

The authors gratefully acknowledge the contributions of the JT-60 team. Also, the authors acknowledge discussions of this study with Dr. M. Sugihara and Dr. T. Takizuka. The authors would like to express their sincere gratitude to Dr. Y. Shimomura, Dr. A. Funahashi, Dr. H. Kishimoto, and Dr. S. Tamura for their continuing encouragement throughout this work. A critical reading of the manuscript by Dr. S. Wolfe is appreciated.

[1] *International Atomic Energy Agency ITER Concept Definition, Vol. 2,* ITER Documentation Series No. 3 (IAEA, Vienna, 1989).
[2] M. Shimada *et al.*, Phys. Rev. Lett. **47**, 796 (1981).
[3] J. C. Deboo *et al.*, Nucl. Fusion **22**, 572 (1982).
[4] R. J. Fonck and R. A. Hulse, Phys. Rev. Lett. **52**, 530 (1984).
[5] E. J. Synakowski *et al.*, Phys. Rev. Lett. **65**, 2255 (1990).
[6] D. L. Hillis *et al.*, Phys. Rev. Lett. **65**, 2382 (1990).
[7] K. Tani *et al.*, in *Proceedings of the Twelfth International Conference on Plasma Physics and Controlled Nuclear Fusion Research, Nice, 1988* (International Atomic Energy Agency, Vienna, 1989), Vol. 2, p. 121.
[8] K. Tobita *et al.*, Nucl. Fusion **31**, 956 (1991).
[9] T. Hirayama *et al.*, J. Nucl. Mater. **145-147**, 854 (1987).
[10] T. Sugie *et al.*, in *Proceedings of the Thirteenth International Conference on Plasma Physics and Controlled Nuclear Fusion Research, Washington, 1990* (International Atomic Energy Agency, Vienna, 1991), Vol. 1, p. 659.
[11] H. B. Gilbody *et al.*, J. Phys. B **4**, 800 (1971).
[12] H. Nakamura *et al.*, Fusion Technology **18**, 578 (1990).
[13] M. Azumi *et al.*, in *Proceedings of the Tenth International Conference on Plasma Physics and Controlled Nuclear Fusion Research, London, 1984* (International Atomic Energy Agency, Vienna, 1985), Vol. 2, p. 131.
[14] K. Yamada *et al.*, Nucl. Fusion **27**, 1203 (1987).
[15] W. Lotz, Astrophys. J., Suppl. Ser. **14**, 207 (1967).